## Appendix Figures

**Appendix Figure S1: Pharmacological inhibition of SPHK2 alleviates DHS-induced genomic and epigenomic instability in human cardiomyocytes.**

**(A)** Micrographs depicting the rescue of DHS-induced genomic instability by 10μM ABC294640, a SPHK2 inhibitor, along with the cardiac marker ACTN2 (in red).

**(B)** Assessment of H3K27ac levels in hCMs by immunostaining, along with the cardiac marker ACTN2 (in red).

**(C)** Representative micrographs depicting the levels of H3K56ac in hCMs by immunostaining, along with the cardiac marker ACTN2 (in red).

**(D)** Micrographs depicting the rescue of DHS-induced genomic instability by indicated concentrations of ABC294640, a SPHK2 inhibitor, along with the cardiac marker ACTN2 (in red).

**(E)** Micrographs depicting the nuclear expression of SPHK2 in hCMs and adult human heart sections, along with the cardiac marker ACTN2 (in red).

**(F)** Curcumin could not rescue the etoposide-induced DNA damage in the human cardiomyocytes, as shown here by staining with anti-γH2A.X antibody (green). Cardiac marker ACTN2 is red.

**(G)** Bar graph depicting the percentage of γH2A.X positive cardiomyocytes nuclei in the indicated conditions. Error bars represent standard error of mean (n=3 biological replicates per condition).

**(H)** Bar graph depicting the numbers of differentially expressed genes (both up and down-regulated) upon DHS exposure of hCMs.

**(I)** Bar graph depicting the prominent Gene Ontologies inferred from the significantly upregulated genes upon DHS exposure of hCMs. Hypergeometric test was used for determining the p-value.

**(J)** Bar graph depicting the prominent Gene Ontologies inferred from the significantly down-regulated genes upon DHS exposure of hCMs. Hypergeometric test was used for determining the p-value.

**(K)** DHS exposure of hCMs do not activate ER and oxidative stress markers, depicted as heatmap.

Data information: ACTN2 is used to specifically label human cardiomyocytes. When not specified, the experiments were conducted in at least 3 biological replicates. Scale bar=10μm.

**Appendix Figure S2: Increase in sphinganine level causes DNA damage in vivo.**

**(A)** Representative micrographs depicting phospho-ATM staining on the ventricle sections for the indicated cohorts. ACTN2 is used to label mouse cardiomyocytes.

**(B)** Quantification of phospho-ATM positive CMs nuclei represented as percentage bar graph. Error bars represent standard error of mean (n=6 animals per condition).

**(C)** Representative micrographs depicting γH2A.X and active-caspase 3 staining on the kidney and liver sections of the indicated cohorts.

**(D)** Quantification of γH2A.X and active-caspase 3 positive cells in kidney and liver samples of the indicated conditions, depicted here as bar graphs. Error bars represent standard error of mean (n=6 animals per condition).

**(E)** Targeted lipidomics approach revealed an increase in DHS levels in heart and serum upon FB1 administration in mice. Lower panel micrographs represents the ventricle view from echocardiography. Error bars represent standard error of mean.

**(F)** Exposure of young adult zebrafish to elevated DHS levels leads to significant increase in DNA damage in cardiomyocytes, visualized here by γH2A.X + nuclei. Curcumin prevents the DHS-induced DNA damage in vivo. MF-20 is used to label zebrafish cardiomyocytes. White arrowheads indicate representative positive signals whereas yellow arrowhead represents nuclei used for line-scan analysis.

**(G)** Florescence intensity line scan of the indicated cardiomyocyte nuclei (marked in yellow) below each micrograph.

**(H)** Bar graph depicting the percentage of γH2A.X positive cardiomyocytes nuclei in the indicated conditions. Error bars represent standard error of mean.

Data information: When not specified, the experiments were conducted in at least 3 biological replicates. For pairwise comparisons Student T-test was performed for the estimation of the statistical significance. Scale bar = 10 μm and for inlets 2μm.

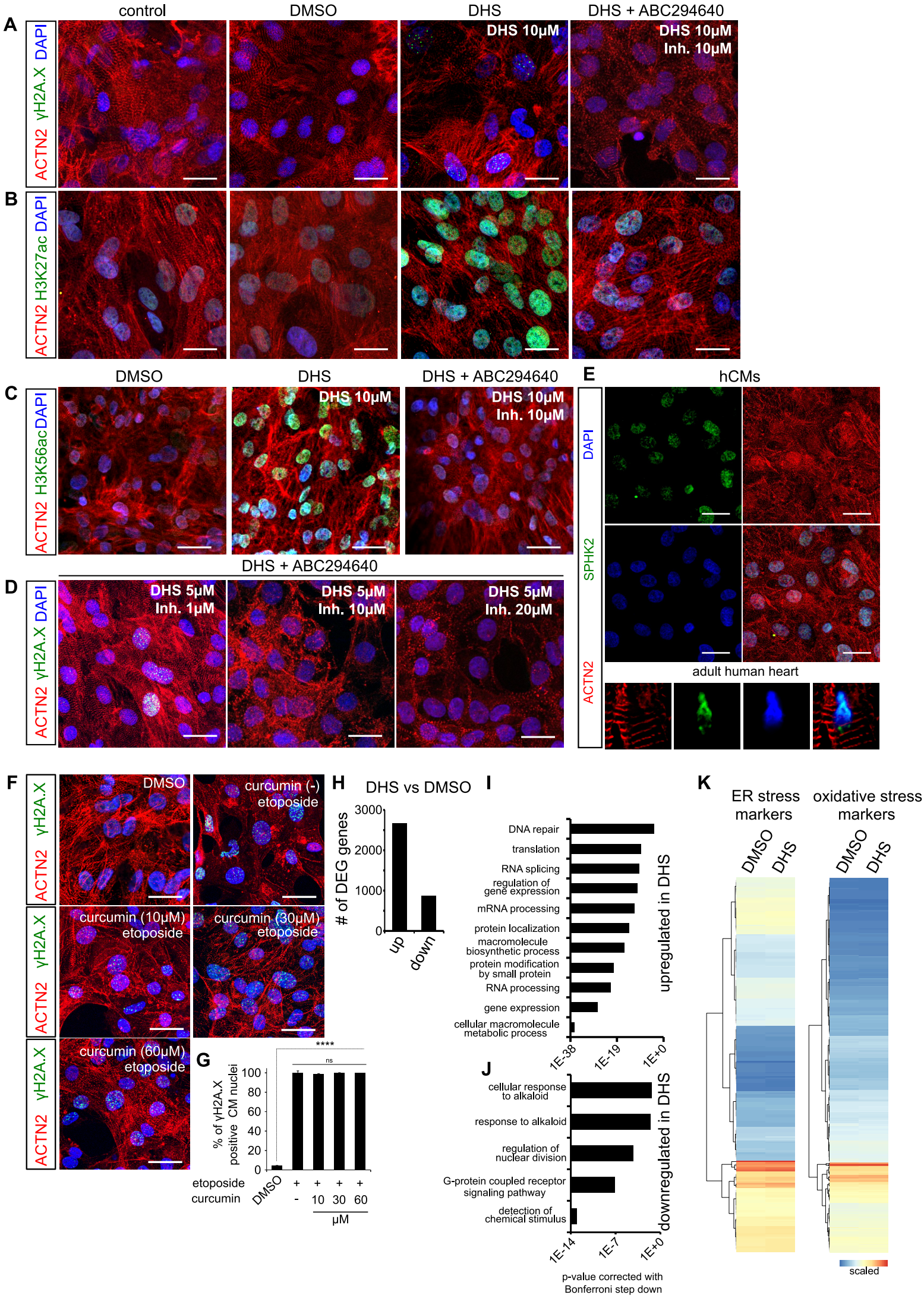
A
control
DMSO
DHS
DHS + ABC294640
ACTN2 γH2A.X DAPI
DHS 10μM
DHS 10μM
Inh. 10μM
B
ACTN2 H3K27ac DAPI
C
DMSO
DHS
DHS + ABC294640
ACTN2 H3K56ac DAPI
DHS 10μM
DHS 10μM
Inh. 10μM
D
DHS + ABC294640
ACTN2 γH2A.X DAPI
DHS 5μM
Inh. 1μM
DHS 5μM
Inh. 10μM
DHS 5μM
Inh. 20μM
E
hCMs
DAPI
SPHK2
ACTN2
adult human heart
F
ACTN2 γH2A.X
DMSO
curcumin (-)
etoposide
curcumin (10μM)
etoposide
curcumin (30μM)
etoposide
curcumin (60μM)
etoposide
G
% of γH2A.X
positive CM nuclei
100
80
60
40
20
0
****
ns
etoposide
curcumin
DMSO
+
-
+
10
+
30
+
60
μM
H
DHS vs DMSO
# of DEG genes
3000
2000
1000
0
up
down
I
DNA repair
translation
RNA splicing
regulation of
gene expression
mRNA processing
protein localization
macromolecule
biosynthetic process
protein modification
by small protein
RNA processing
gene expression
cellular macromolecule
metabolic process
upregulated in DHS
1E-38
1E-19
1E+0
J
cellular response
to alkaloid
response to alkaloid
regulation of
nuclear division
G-protein coupled receptor
signaling pathway
detection of
chemical stimulus
downregulated in DHS
1E-14
1E-7
1E+0
p-value corrected with
Bonferroni step down
K
ER stress
markers
oxidative stress
markers
DMSO
DHS
DMSO
DHS
scaled

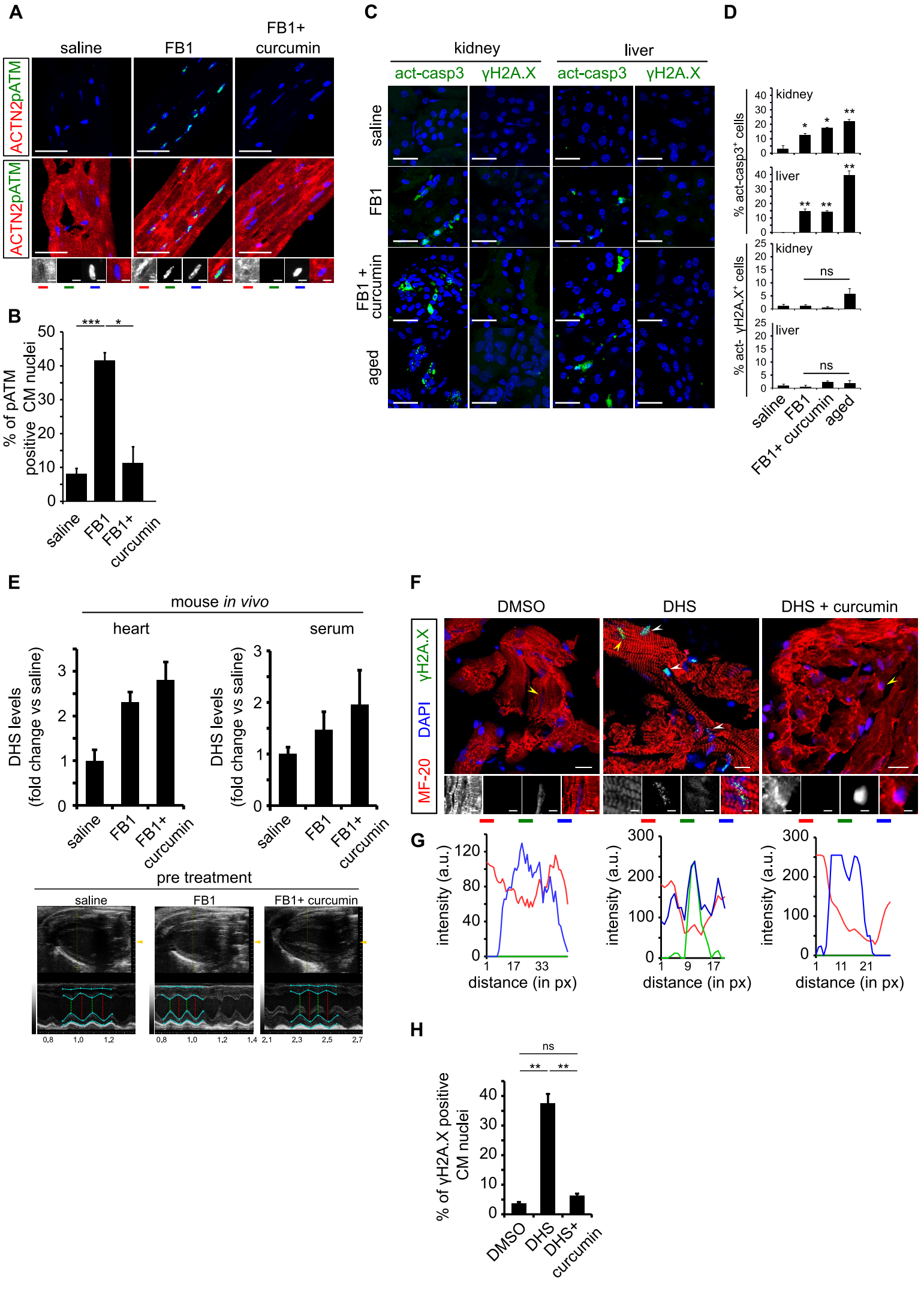
A
saline
FB1
FB1+ curcumin
ACTN2pATM
ACTN2pATM
B
% of pATM positive CM nuclei
***
*
saline
FB1
FB1+ curcumin
C
kidney
liver
act-casp3
γH2A.X
act-casp3
γH2A.X
saline
FB1
FB1 + curcumin
aged
D
% act-casp3+ cells
kidney
liver
% act- γH2A.X+ cells
kidney
liver
ns
ns
saline
FB1
FB1+ curcumin
aged
E
mouse in vivo
heart
serum
DHS levels (fold change vs saline)
DHS levels (fold change vs saline)
saline
FB1
FB1+ curcumin
saline
FB1
FB1+ curcumin
pre treatment
saline
FB1
FB1+ curcumin
F
DMSO
DHS
DHS + curcumin
MF-20
DAPI
γH2A.X
G
intensity (a.u.)
distance (in px)
intensity (a.u.)
distance (in px)
intensity (a.u.)
distance (in px)
H
ns
**
**
% of γH2A.X positive CM nuclei
DMSO
DHS
DHS+ curcumin